

# lncRNA PITPNA-AS1 promotes cell proliferation and metastasis in hepatocellular carcinoma by upregulating PDGFD

Jianguo Yao<sup>1</sup>, Xiaojian Liu<sup>1</sup>

<sup>1</sup>Department of Surgery, Tongxiang First People's Hospital, Tongxiang 314500, Zhejiang, P.R. China

**Correspondence to:** Xiaojian Liu; email: [xiaoj5l@163.com](mailto:xiaoj5l@163.com), <https://orcid.org/0000-0003-0592-191X>

**Keywords:** hepatocellular carcinoma, lncRNA, PITPNA-AS1, miR-363-5p, PDGFD

**Received:** October 10, 2021

**Accepted:** February 11, 2023

**Published:** March 2, 2023

**Copyright:** © 2023 Yao and Liu. This is an open access article distributed under the terms of the [Creative Commons Attribution License](https://creativecommons.org/licenses/by/3.0/) (CC BY 3.0), which permits unrestricted use, distribution, and reproduction in any medium, provided the original author and source are credited.

## ABSTRACT

Hepatocellular carcinoma (HCC) ranks high in morbidity and mortality among notorious malignancies because of the lack of effective biomarkers and treatments. lncRNA PITPNA antisense RNA 1 (PITPNA-AS1) plays an oncogenic role in HCC, yet the mechanistic basis remains unprobed. Here using Bioinformatics and PCR analyses, we validated that PITPNA-AS1 expression was significantly increased in HCC. The levels of PITPNA-AS1 in tumors were reversely correlated with the prognosis in HCC patients. Downregulation of PITPNA-AS1 inhibited malignant activities of HCC cells. Next, we elucidated that PITPNA-AS1 acts as a competing endogenous RNA (ceRNA) to sponge miR-363-5p, thereby regulating the expression of platelet-derived growth factor-D (PDGFD). Moreover, the suppression of HCC cell activities by PITPNA-AS1 downregulation can be removed by PDGFD overexpression or miR-363-5p inhibition. Collectively, our work reveals the involvement of the PITPNA-AS1/miR-363-5p/PDGFD regulatory axis in HCC progression.

## INTRODUCTION

Hepatocellular carcinoma (HCC) prevalently occurs worldwide with astonishing death rate [1–3]. Despite limited advances made to HCC treatment recently, the survival rate of patients within five years is still poor largely because of the high propensity of metastasis [3–5]. Therefore, identification of novel biomarkers and effective pharmaceutical targets is urgently needed.

In the human genome, more than 75% of genomic regions code for non-coding RNAs [6]. Long non-coding RNAs (lncRNAs) are typically 200 nucleotides in length and are involved in transcriptional and translational regulation of gene expression, as well protein degradation [7]. Recently, novel lncRNAs have been identified as critical regulators in HCC [8, 9], potentiating lncRNAs as biomarkers and pharmaceutical targets for HCC. For example, lncRNA AC099850.3 regulates the PRR11/PI3K/AKT axis to promote HCC proliferation and invasion and is associated with the prognosis in patients [10].

Moreover, novel lncRNA AL033381.2 can upregulate PRKRA to promote HCC progression [11]. However, the impact of dysregulation of lncRNAs on HCC is unknown [12, 13].

In general, cytoplasmic lncRNAs function as competing endogenous RNAs (ceRNA) to sponge miRNAs, thereby regulating functional gene expressions. This mechanism is known as the lncRNA-miRNA-mRNA network [14, 15]. This network has been implicated in HCC progression. For example, lncRNA ILF3-AS1 promotes cell migration and invasion and the EMT process in HCC by activating the Notch pathway through the miR-628-5p/MEIS2 axis [8]. In addition, lncRNA CYTOR targets the microRNA-125a-5p/LASP1 axis to promote HCC proliferation [16]. More recently, PITPNA-AS1 was reported to sponge miR-876-5p to accelerate HCC and cervical cancer progression [17, 18]. Similarly, PITPNA-AS1 can modulate the miR-448/ROCK1 axis to promote HCC progression [19]. These studies suggest that PITPNA-AS1 can regulate HCC progression through multiple

pathways in HCC. However, whether PITPNA-AS1 regulates HCC progression through sponging other miRNAs remains unclear.

microRNAs (miRNAs) comprise approximately 22 nucleotides, belonging to non-coding RNA families. They typically act as a translation suppressor by binding to the 3' untranslated regions (UTR) of target mRNAs. Recently, the pathogenic roles of miRNAs in HCC have been revealed. For instance, miR-124-3p.1 sensitizes the response of HCC cells to sorafenib by regulating FOXO3a levels through targeting AKT2 and SIRT1 [20], and miR-221-3p targets LIFR to regulates HCC cell performance [21]. It has been revealed that low levels of miR-363 expression are closely associated with carcinogenesis, and metastasis as well [22]. Moreover, it was predicted that the expression level of miR-363-5p was significantly downregulated in HCC tumor endothelial cells [23]. Also, expression of miR-363-5p was demonstrated to be downregulated in other tumors including nasopharyngeal carcinoma and breast cancer [24, 25]. However, the intrinsic mechanism of

miR-363-5p regulation in HCC has not been fully elucidated. Here, by analyzing the TCGA database and PCR validation in human HCC tissue, we discovered the association of PITPNA-AS1 expression levels with was the prognosis in patients with HCC. Moreover, we delineated the mechanistic basis of the contribution of PITPNA-AS1 to HCC progression.

## RESULTS

### Upregulation of PITPNA-AS1 associates with poor prognosis of HCC

The cancer genome atlas (TCGA) dataset (ENSG00000236618) was downloaded from GEPIA (<http://gepia.cancer-pku.cn/>), and the expression pattern of PITPNA-AS1 was evaluated. The results revealed the upregulation of PITPNA-AS1 in HCC and the association with the poor survival of the patients (Figure 1A). We then examined the relative PITPNA-AS1 expression levels in dissected HCC tumor tissues.

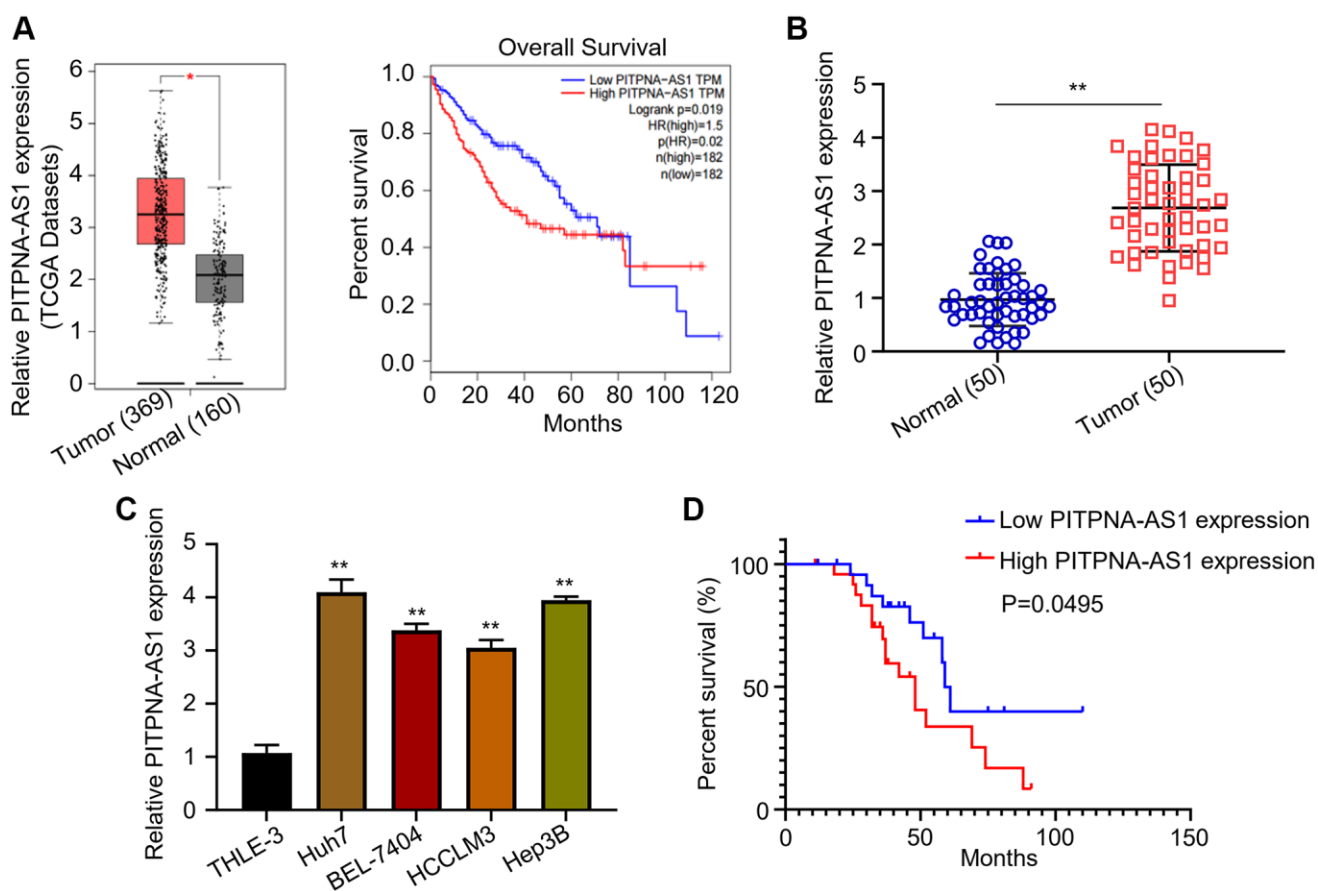


**Figure 1. PITPNA-AS1 is overexpressed in HCC and associates with poor prognosis.** (A) Relative mRNA level of PITPNA-AS1 in TCGA datasets was analyzed using GEPIA. (B) Relative mRNA level of PITPNA-AS1 in 50 pairs of tumor tissues and adjacent normal tissues were assessed using qRT-PCR. (C) Relative mRNA level of PITPNA-AS1 in HCC cell lines (Huh7, BEL-7404, HCCLM3, Hep3B) and the control cell line, THLE-3. (D) Correlation of PITPNA-AS1 expression levels with patients' survival was evaluated by the Kaplan-Meier analysis. \* $P < 0.05$ , \*\* $P < 0.01$ .

**Table 1. Clinicopathological data of the 50 HCC patients.**

| Clinical parameters           | Total | High expression (25) | Low expression (25) | $\chi^2$ | <i>P</i> value |
|-------------------------------|-------|----------------------|---------------------|----------|----------------|
| <b>Gender</b>                 |       |                      |                     |          |                |
| Male                          | 22    | 12                   | 10                  | 0.325    | 0.569          |
| Female                        | 28    | 13                   | 15                  |          |                |
| <b>Age (Year)</b>             |       |                      |                     |          |                |
| <50                           | 23    | 14                   | 9                   | 2.013    | 0.156          |
| ≥50                           | 27    | 11                   | 16                  |          |                |
| <b>HBeAg</b>                  |       |                      |                     |          |                |
| Negative                      | 39    | 20                   | 19                  | 0.117    | 0.733          |
| Positive                      | 11    | 5                    | 6                   |          |                |
| <b>HBVDNA (IU/mL)</b>         |       |                      |                     |          |                |
| <2000                         | 31    | 16                   | 15                  | 0.085    | 0.771          |
| ≥2000                         | 19    | 9                    | 10                  |          |                |
| <b>Number of Node</b>         |       |                      |                     |          |                |
| Single                        | 30    | 17                   | 13                  | 1.333    | 0.249          |
| ≥2                            | 20    | 8                    | 12                  |          |                |
| <b>Macrovascular invasion</b> |       |                      |                     |          |                |
| Negative                      | 20    | 5                    | 15                  | 8.333    | 0.004**        |
| Positive                      | 30    | 20                   | 10                  |          |                |
| <b>Child-Pugh class</b>       |       |                      |                     |          |                |
| A                             | 40    | 20                   | 20                  | 0        | 1              |
| B                             | 10    | 5                    | 5                   |          |                |
| <b>AFP (ng/mL)</b>            |       |                      |                     |          |                |
| <400                          | 33    | 15                   | 18                  | 0.802    | 0.37           |
| ≥400                          | 17    | 10                   | 7                   |          |                |
| <b>Differentiation</b>        |       |                      |                     |          |                |
| Well                          | 15    | 5                    | 10                  | 2.381    | 0.123          |
| Moderately poorly             | 35    | 20                   | 15                  |          |                |
| <b>Largest tumor size</b>     |       |                      |                     |          |                |
| <3 cm                         | 13    | 6                    | 7                   | 2.348    | 0.309          |
| 3–5 cm                        | 20    | 8                    | 12                  |          |                |
| >5 cm                         | 17    | 11                   | 6                   |          |                |
| <b>Tumor stage</b>            |       |                      |                     |          |                |
| I + II                        | 28    | 10                   | 18                  | 5.195    | 0.023*         |
| III + IV                      | 22    | 15                   | 7                   |          |                |

\* $P < 0.05$ ; \*\* $P < 0.01$ .

Consistently, qRT-PCR results found the upregulation of PITPNA-AS1 in the tumor tissues (Figure 1B). Similarly, the PITPNA-AS1 expression levels in the four HCC cell lines (Huh7, BEL-7404, HCCLM3, and Hep3B) were higher than in the normal human hepatic epithelial cell line, THLE-3 (Figure 1C). Next, based on the medium expression value, the 50 patients were assigned ( $n = 25$ ) into PITPNA-AS1 low- and high-expression groups. As shown in Table 1, a correlation analysis revealed that expression levels of PITPNA-AS1 positively associates with macrovascular invasion ( $p = 0.04$ ) and tumor stages ( $p = 0.023$ ). In addition,

the Kaplan-Meier analysis showed a reverse correlation of high PITPNA-AS1 expression levels with the overall survival rates of the patients (Figure 1D).

#### **PITPNA-AS1 promotes proliferation, migration and invasion of HCC**

To probe the role of PITPNA-AS1 in HCC progression, we silenced the expression of PITPNA-AS1 using two short hairpin RNAs in Huh7 and Hep3B cells with high PITPNA-AS1 expression (Figure 2A). CCK-8 assay

showed that PITPNA-AS1 knockdown inhibited the growth of Huh7 and Hep3B cells in a time-dependent manner (Figure 2B). Moreover, the transwell assay revealed that PITPNA-AS1 knockdown strongly suppressed the migration and invasion of Huh7 and

Hep3B cells, but sh-NC did not (Figure 2C and 2D). Consistently, the cells with PITPNA-AS1 knockdown exhibited downregulation of the mesenchymal marker N-cadherin and MMP9, whereas upregulation of epithelial marker E-cadherin (Figure 2E). Collectively,

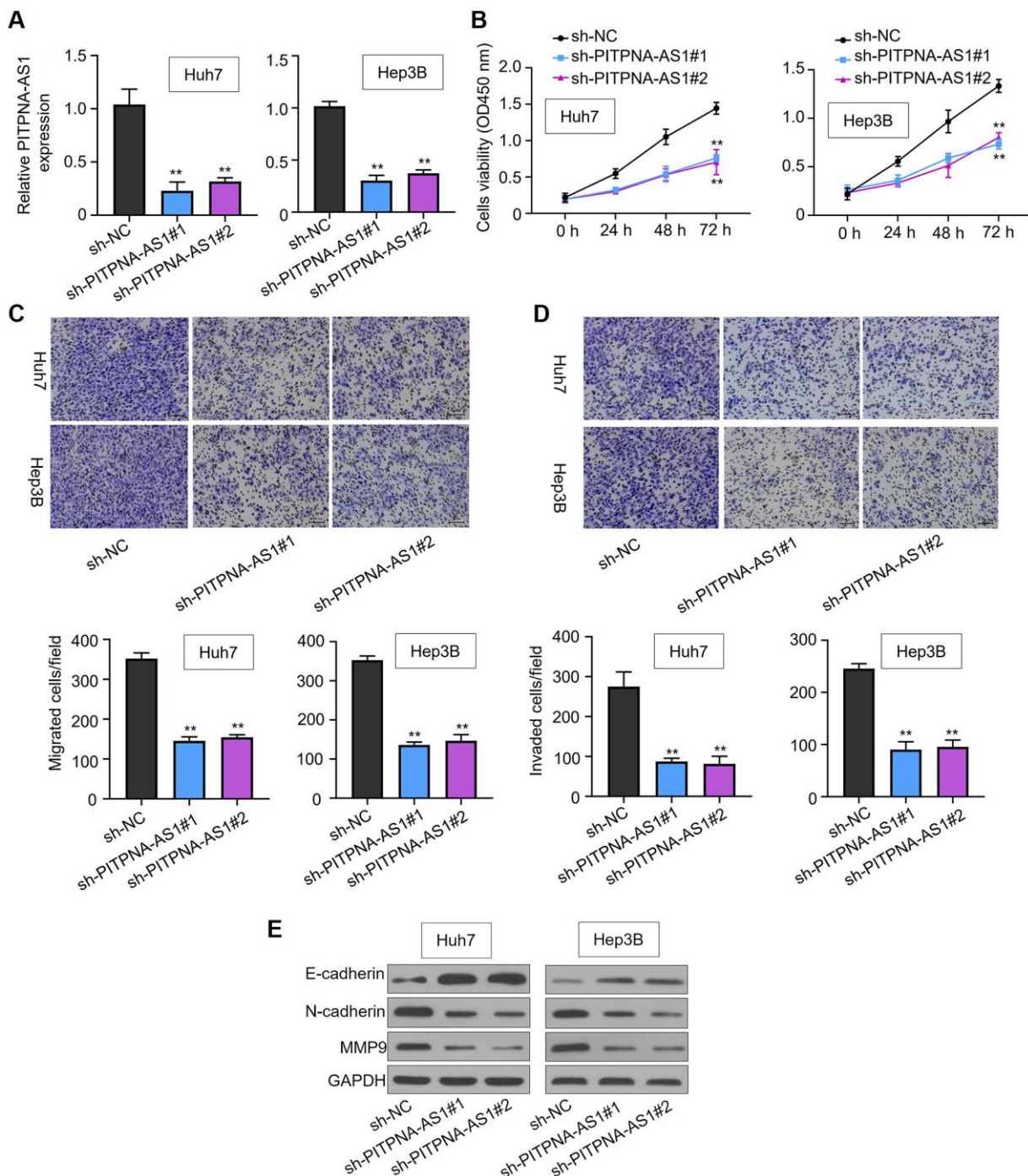


**Figure 2. PITPNA-AS1 promotes cell proliferation, migration, and invasion in HCC.** (A) PITPNA-AS1 mRNA levels in Huh7 and Hep3B cells transfected with sh-NC, sh-PITPNA-AS1#1, or sh-PITPNA-AS1#2 was determined by qRT-PCR. (B) Proliferation of Huh7 and Hep3B cells transfected with sh-NC, sh-PITPNA-AS1#1, or sh-PITPNA-AS1#2 was measured by the CCK-8 assay. (C and D) Migration and invasion capabilities of Huh7 and Hep3B transfected with sh-NC, sh-PITPNA-AS1#1, or sh-PITPNA-AS1#2 was assessed by the transwell assay. Magnification rate, 200 $\times$ . (E) EMT-related protein levels in Huh7 and Hep3B cells transfected with sh-NC, sh-PITPNA-AS1#1, or sh-PITPNA-AS1#2 were determined by western blot. \*\* $P < 0.01$ .

the above data suggest that PITPNA-AS1 positively contributed to invasive capacity of HCC cells.

### PITPNA-AS1 sponges miR-363-3p in HCC cells

StarBase3.0 (<http://starbase.sysu.edu.cn/>) was used to search for the potential miRNA potentially targeted by PITPNA-AS1. The online algorithm suggested that miR-363-5p ranked the highest among the predicted miRNAs that could bind to PITPNA-AS1 (Figure 3A). Then we quantified the level of miR-363-5p and found that the expression of miR-363-5p was higher in normal cells versus HCC cell lines (Figure 3B). Further, the cells transfected with miR-363-5p exhibited lower luciferase activity than in the cells transfected with wide-type PITPNA-AS1 (PITPNA-AS1 WT) (Figure 3C). However, the cells transfected with PITPNA-AS1 mutant (PITPNA-AS1 MUT) with

mutated miR-363-5p binding site showed comparable luciferase activity with control cells (Figure 3C). Besides, the RIP assay showed that PITPNA-AS1 was coimmunoprecipitated with the biotin-labeled miR-363-5p probe (Figure 3D). These results implicated that PITPNA-AS1 directly bind to miR-363-5p. Consistently, we observed that knockdown of PITPNA-AS1 in Huh7 and Hep3B cells resulted in upregulation of miR-363-5p (Figure 3E).

### PDGFD is a direct target of miR-363-3p

Further, StarBase3.0 was employed to predict the potential gene targeted by miR-363-5p. The prediction suggested platelet-derived growth factor D (PDGFD) as a target for miR-363-5p (Figure 4A). As shown by the luciferase assay, miR-363-5p could interact with PDGFD to reduce the luciferase activity of PDGFD WT

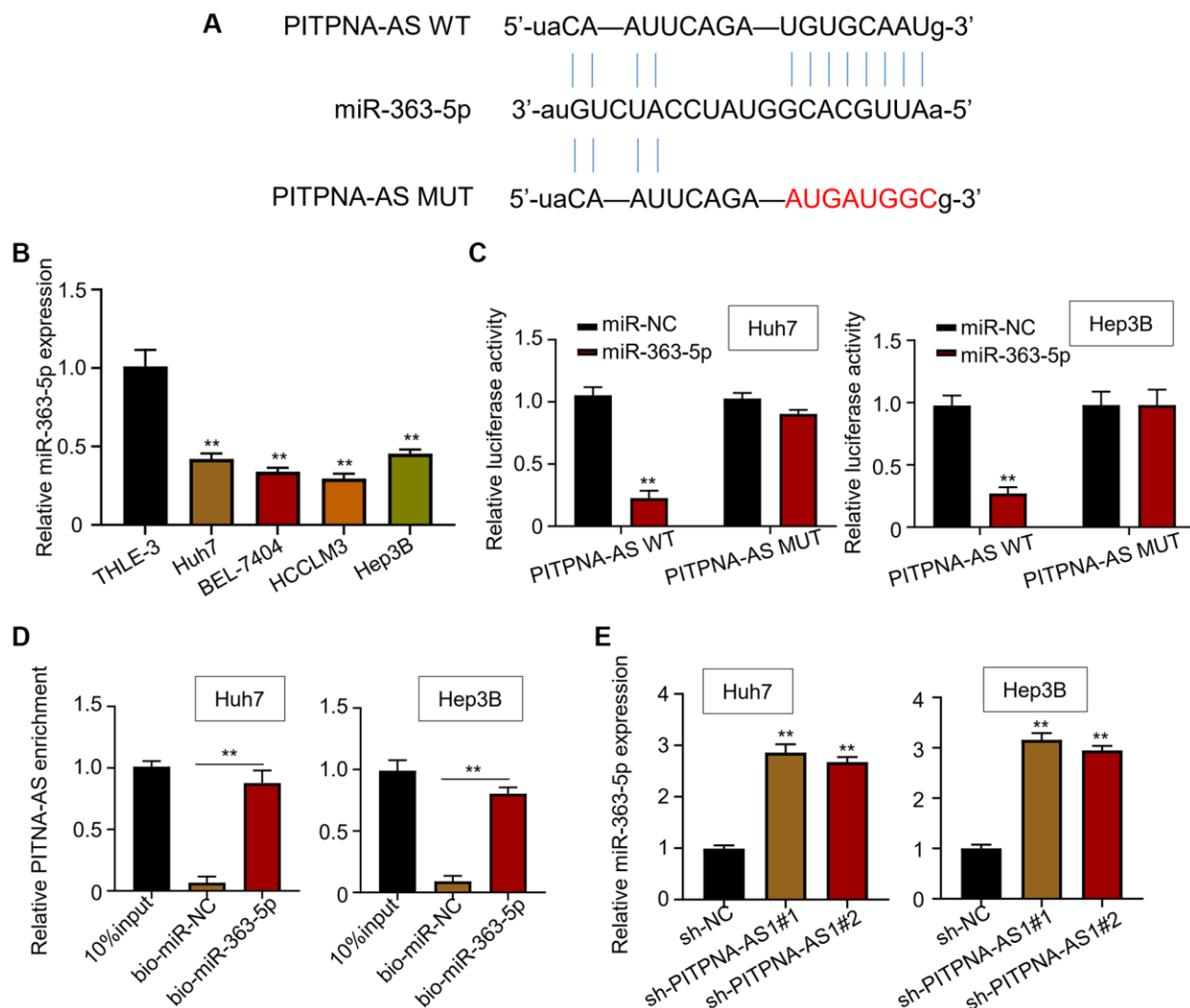


**Figure 3. PITPNA-AS1 sponges miR-363-3p in HCC cells.** (A) A binding motif of miR-363-5p within PITPNA-AS1 predicted by StarBase3.0. (B) Relative mRNA level of miR-363-5p in four HCC cell lines (Huh7, BEL-7404, HCCLM3, and Hep3B) and the control cell line, THLE-3. (C) Luciferase activity in Huh7 and Hep3B cells transfected with miR-NC or miR-363-5p mimic. (D and E) Interaction between PITPNA-AS1 and miR-363-5p was determined by RIP and luciferase reporter assays. \*\* $P < 0.01$ .

but did not reduce the activity of PDGFD MUT with mutated binding site was in Huh7 and Hep3B cells (Figure 4B). Moreover, transfection of miR-363-5p mimics dramatically decreased PDGFD transcript and protein levels of (Figure 4C). In addition, miR-363-5p inhibitor treatment could rescue the downregulation of PDGFD caused by sh-PITPNA-AS1#1 (Figure 4D and 4E).

### PITPNA-AS1 promotes HCC progression through the miR-363-3p/PDGFD axis

To explore whether PITPNA-AS1 promotes HCC progression by modulating the miR-363-5p/PDGFD

axis, we applied miR-363-5p inhibitor or overexpressed PDGFD in sh-PITPNA-AS1#1-transfected HCC cells. The CCK-8 assay showed that either miR-363-5p inhibition or PDGFD overexpression could eliminate the inhibitory effect in sh-PITPNA-AS1#1 transfected cells (Figure 5A and 5B). Further, the transwell assay also confirmed the restoration of the impaired cell invasion by either miR-363-5p inhibition or PDGFD overexpression (Figure 5C and 5D). Consistently, miR-363-5p inhibition or PDGFD overexpression reversed the downregulation of N-cadherin and MMP9 and the upregulation of E-cadherin in PITPNA-AS1- knockdown HCC cells (Figure 5E). These data indicate that PITPNA-AS1

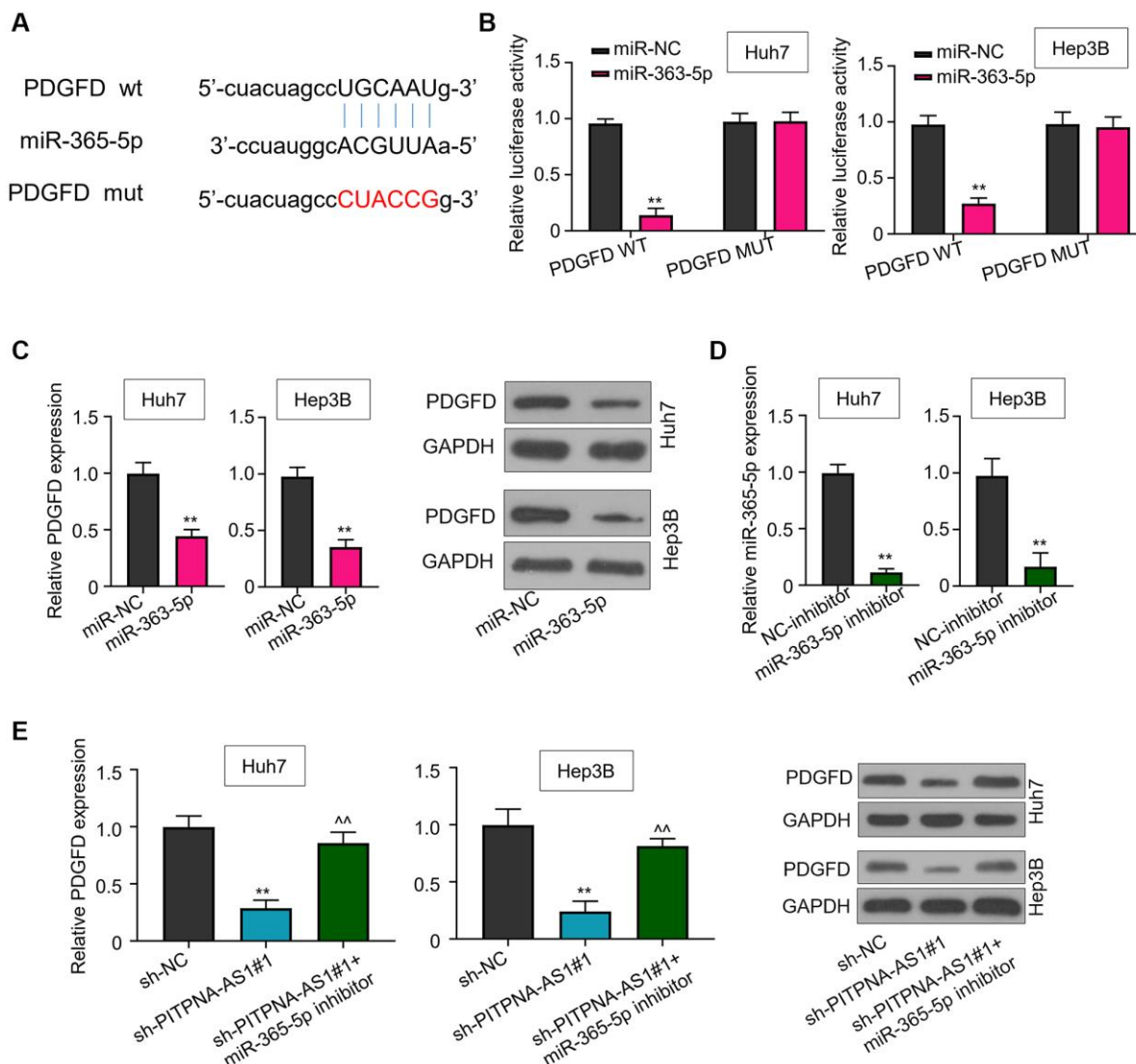


**Figure 4. PDGFD is a downstream target of miR-363-3p.** (A) A binding motif of PDGFD within miR-363-3p predicted byStarBase3.0 (<http://starbase.sysu.edu.cn/>). (B) Luciferase activity in Huh7 and Hep3B cells transfected with miR-NC or miR-363-5p mimic. (C) PDGFD levels in Huh7 and Hep3B cells treated with NC-inhibitor or miR-363-5p inhibitor. (D) Relative expression of miR-363-5p in Huh7 and Hep3B cells treated with NC-inhibitor or miR-363-5p inhibitor. (E) PDGFD expression levels in Huh7 and Hep3B cells transfected with sh-NC, sh-PITPNA-AS1#1, or sh-PITPNA-AS1#1+miR-363-5p inhibitor were quantified by qRT-PCR and western blot. \*\* $P < 0.01$ , compared to the sh-NC group; ^^ $P < 0.01$ , compared to the sh-PITPNA-AS1#1 group.

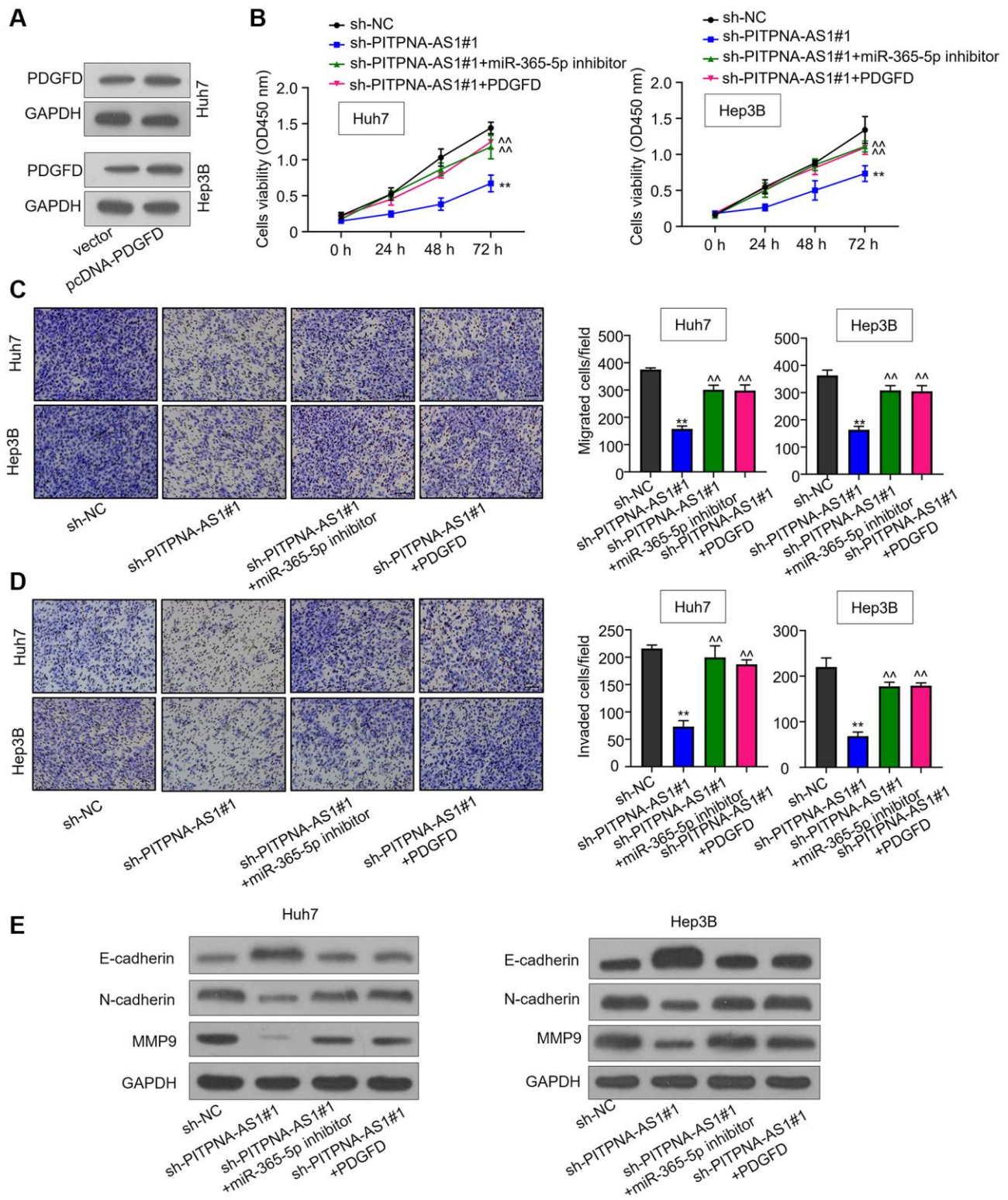


**Figure 5. PITPNA-AS1 promotes HCC progression through the miR-363-3p/PDGFD axis.** (A) Protein level of PDGFD in Huh7 and Hep3B cells transfected with pcDNA3.1-PDGFD. (B) Cell proliferation of HCC cells transfected with sh-NC, sh-PITPNA-AS1#1, sh-PITPNA-AS1#1+miR-363-5p inhibitor, or sh-PITPNA-AS1#1+miR-363-5p inhibitor + pcDNA3.1-PDGFD was examined by the CCK-8 assay. (C and D) Cell migration and invasion of Huh7 and Hep3B cells transfected with sh-NC, sh-PITPNA-AS1#1, sh-PITPNA-AS1#1+miR-363-5p inhibitor, or sh-PITPNA-AS1#1+miR-363-5p inhibitor+pcDNA3.1-PDGFD was investigated by the transwell assay. \*\* $P < 0.01$ , compared to the sh-NC group; ^^ $P < 0.01$ , compared to the sh-PITPNA-AS1#1 group. (E) EMT-related protein levels of Huh7 and Hep3B cells transfected with sh-NC, sh-PITPNA-AS1#1, sh-PITPNA-AS1#1+miR-363-5p inhibitor, or sh-PITPNA-AS1#1+miR-363-5p inhibitor+pcDNA3.1-PDGFD were determined by western blot.

promotes HCC progression through the miR-363-3p/PDGFD axis.

### Knockdown of PITPNA-AS1 inhibits HCC progression *in vivo*

To further determine the function of PITPNA-AS1, we used the Huh7 cells, which were transfected with sh-PITPNA-AS1#1, to establish xenograft nude mice models. We observed that PITPNA-AS1 knockdown significantly suppressed tumor growth in mice as compared to the control group. The tumor in the xenograft nude mice was about 2 cm in diameter, whereas the diameter of the tumor in the control mice was only about 1 cm (Figure 6A). Tumor weights were also reduced in the xenograft nude mice models (Figure 6B). Moreover, we used IHC to investigate the expression levels of classic tumor biomarkers, including PDGFD, Ki-67, E-cadherin, N-cadherin, and  $\beta$ -catenin. Of these, PDGFD, Ki-67, N-cadherin, and  $\beta$ -catenin were downregulated, while E-cadherin was upregulated in the sh-PITPNA-AS1 group (Figure 6C). Figure 7 reports a schematic diagram elucidating the promotion of HCC progression by the PITPNA-AS1/miR-363-5p/PDGFD axis (Figure 7).

## DISCUSSION

Increasing evidence has suggested that lncRNAs are key regulators in solid tumors with aberrant stages,

including HCC [26, 27], potentiating lncRNAs as effective biomarkers. However, the relationship between the lncRNAs and tumorigenesis is still obscure [12, 13]. The interaction of lncRNAs and miRNAs and their roles in tumorigenesis as biomarkers have become a major research interest [28]. Thus, understanding their interaction is necessary for developing new diagnosis and therapy for cancers. It was reported that PITPNA-AS1 inhibits miR-876-5p, thereby upregulating WNT5A to promote HCC progression [17, 18]. Yet the exact regulatory mechanism of PITPNA-AS1 in HCC is largely unclear. In oral squamous cell carcinoma, lncRNA MCM3AP-AS1 inhibits miR-363-5p expression to promote cell proliferation, migration and invasion [29]. Similarly, lncRNA FOXD2-AS1 downregulates miR-363-5p to aggravates nasopharyngeal carcinoma progression [25]. In contrast, a close association of low miR-363-5p expression levels with better overall survival in patients with HCC have been reported [23, 30]. Therefore, miR-363-5p appears to be a ubiquitous miRNA involved in tumor progression. However, whether PITPNA-AS1 may interact with miR-363-5p in HCC remains to be explored. Platelet-derived growth factor D (PDGFD) has been implicated in the EMT phenotype of HCC [31]. PDGFD could crosstalk with miRNAs in various cancer types [32–34]. Although PDGFD is widely implicated in tumorigenesis, the exact mechanism by which

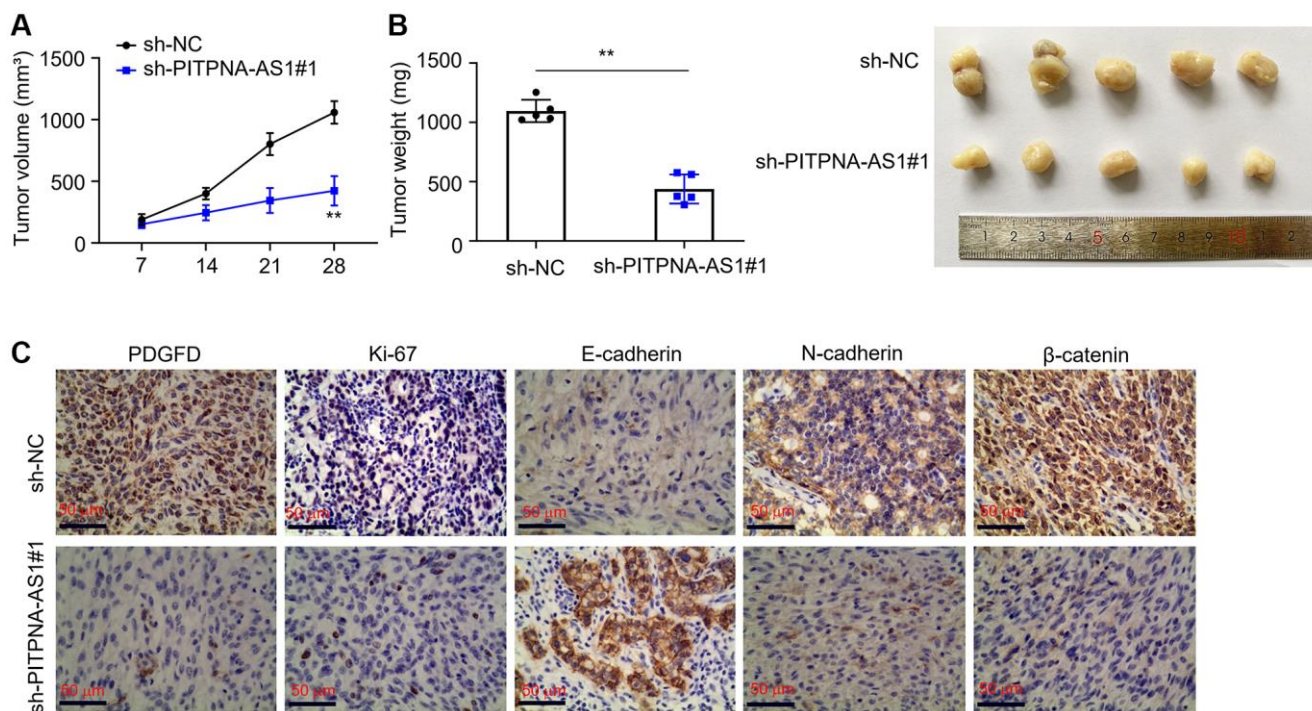


**Figure 6. Knockdown of PITPNA-AS1 inhibits HCC progression.** (A and B) Tumor volume and weight in xenograft nude models. (C) Expression levels of PDGFD,  $\beta$ -catenin, Ki67, E-cadherin, and N-cadherin were determined by IHC. \*\* $P < 0.01$ .

PDGFD regulates HCC progression remain mysterious.

In the current study, we characterized the downstream gene targeted by PITPNA-AS1 and miR-363-5p. The aberrant expression of PITPNA-AS1 was strongly related to the overall survival of HCC patients. The growth and invasion capacity of HCC cells were inhibited by PITPNA-AS1 knockdown. Further, we studied the mechanistic basis of PITPNA-AS1's regulation on HCC. The bioinformatic analysis predicted the interaction between PITPNA-AS1 and miR-363-5p, and miR-363-5p and PDGFD. RIP and luciferase assays confirmed the complementary interaction between them in HCC. Additionally, we demonstrated that

downregulation of PITPNA-AS1 could inhibit the tumor-promoting effect rescued by inhibiting miR-363-5p or overexpressing PDGFD, indicating that PITPNA-AS1 accelerates HCC development by downregulating miR-363-5p and upregulating PDGFD expression.

We demonstrate the upregulation of PITPNA-AS1 in HCC and its correlation with poor prognosis in patients. Mechanically, PITPNA-AS1 sponges miR-363-5p to upregulate PDGFP, thereby accelerating HCC progression. Collectively, our data indicate that PITPNA-AS1 exerts tumor-promoting effects in HCC progression and that PITPNA-AS1/miR-363-5p/PDGFD axis may be a good pharmaceutical target for HCC treatment.

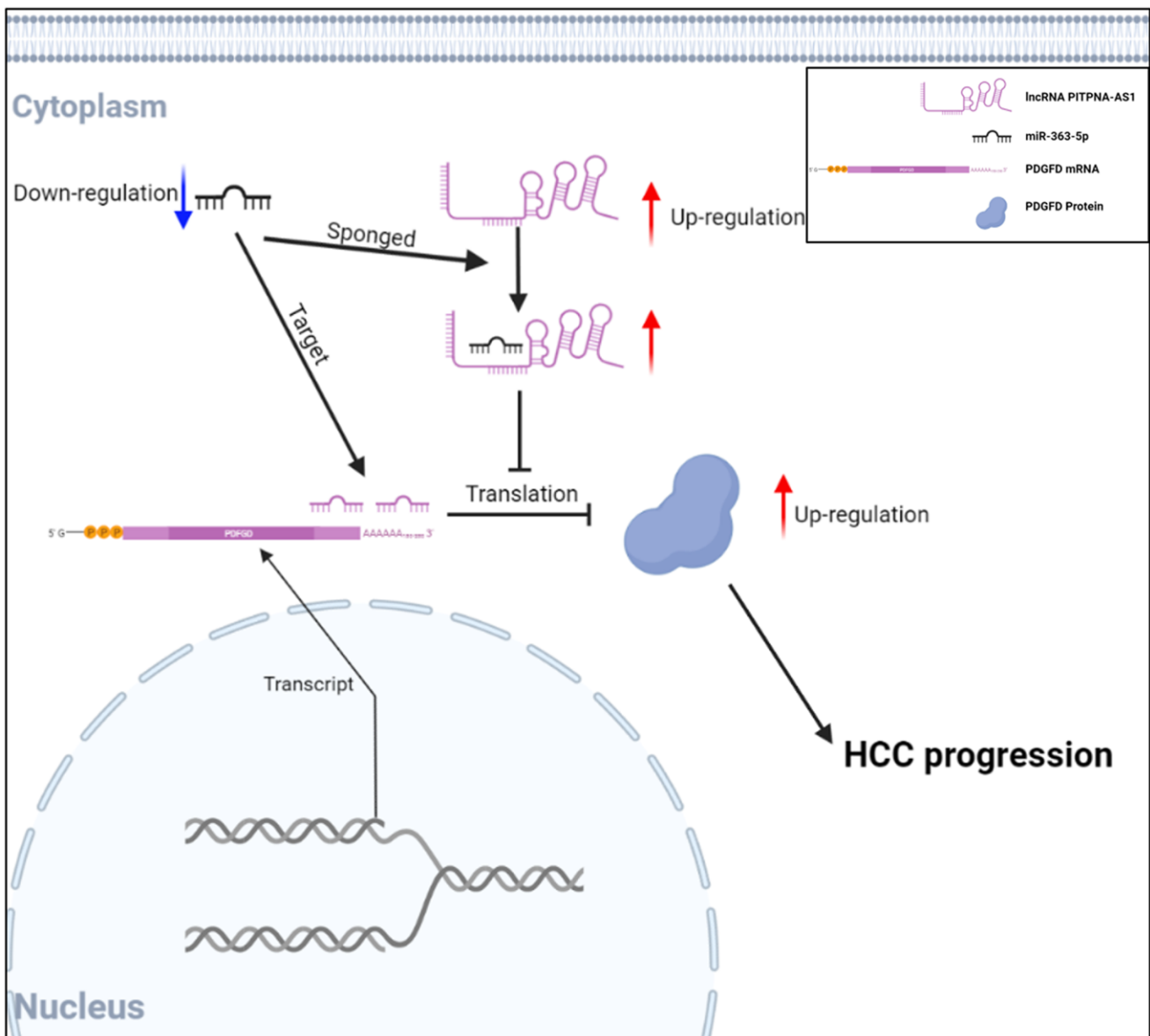


Figure 7. The schematic diagram showing the function of PITPNA-AS1/miR-363-5p/PDGFD axis in HCC progression.

## MATERIALS AND METHODS

### Clinical samples

HCC tumor tissues and the paired adjacent non-cancerous tissues ( $n = 50$ ) were surgically dissected from the HCC patients who had not received any preoperative therapies at the Tongxiang First People's Hospital between 2016 and 2019. The samples were snap frozen in liquid nitrogen. The demographic and clinicopathological features of the patients were listed in Table 1. The study was approved by the ethical committee of the Tongxiang First People's Hospital.

### Cell lines

ATCC provided the human normal hepatic epithelial cell line (THLE-3) and the four HCC cell lines (Huh7, BEL-7404, HCCLM3, and Hep3B) which were cultured in Dulbecco's modified Eagle's medium (DMEM) (Gibco, USA).

### Cell transfection

Short hairpin RNA (shRNA) for RNA interference was synthesized by Gema supersilencing™ shRNA expression vector system. Bbs I and BamH I were used for cloning shRNA sequence into the vector, and Neomycin tolerance gene was used to screen positive transfection colonies. miR-363-5p mimics, inhibitor, and NC negative controls were purchased from GeneCopoeia (Guangdong, China). To overexpress PDGFD, the full length of PDGFD was cloned into pcDNA3.1 (Invitrogen, CA, USA) plasmid to generate pcDNA3.1-PDGFD. Cell transfection was implanted using Lipofectamine® 2000 (Invitrogen, CA, USA) at room temperature for 48 h.

### Quantitative reverse transcription-polymerase chain reaction

RNA extraction was performed with Trizol reagent (Invitrogen, CA, USA). The complementary DNA (cDNA) was prepared using the PrimeScript RT reagent kit (Takara, Japan). qRT-PCR was performed using SYBR Green Real-Time PCR Master Mix with the ABI 7900 Fast Thermal Cycler (Thermo Fisher Scientific, MA, USA). GAPDH was used as a reference gene for quantifying lncRNA and mRNA, and U6 was used for quantifying miRNA. The PCR program was: pre-denaturation at 95°C for 1 min; 35 cycles of 10 s denaturation at 95°C, 15 s annealing at 60°C, and 10 s elongation at 72°C; post-elongation at 72°C for 2 min. The calculation of the relative gene

expression was performed as per the  $2^{\Delta\Delta Ct}$  method. The primers were listed below:

GAPDH: F: 5'-TGCACCACCAACTGCTTAGC-3'  
R: 5'-GGCATGCACTGTGGTCATGAG-3'  
U6: F: 5'-CTCGCTTCGGCAGCAC-3'  
R: 5'-AACGCTTCACGAATTTGCGT-3'  
PITPNA-AS1: F: 5'-GCAGGGTGGATAAAGAGGA-3'  
R: 5'-CCTACTGACAGGATGTCCT-3'  
miR-363-5p: F: 5'-CGAATTGCACGGTATCCATCT-3'  
R: 5'-GTGCAGGGTCCGAGGT-3'  
PDGFD: F: 5'-CCCAGGAATTACTCGGTCAA-3'  
R: 5'-ACAGCCACAATTTCTCCAC-3'

### Bioinformatic analysis

The binding site of miR-363-5p in PITPNA-AS1 and the binding site of PDGFD in miR-363-5p was screened by a web-based bioinformatic tool, StarBase 3.0 (<http://starbase.sysu.edu.cn/>) [35].

### Cell counting kit-8 (CCK-8) assay

The cells ( $3 \times 10^3$ /well) with different treatments were plated into 96-well plates. Then, each well was added with CCK-8 solution (10  $\mu$ l) (Dojindo, Japan) at 0 h, 24 h, 48 h, and 72 h. After incubation for 1 h at 37°C, the 450 nm wavelength absorbance was detected with Synergy H4 Hybrid Reader (BioTek, VT, USA).

### Transwell assay

To perform the invasion assay,  $2 \times 10^5$  cells suspended in 250  $\mu$ l of serum-free medium were applied to the upper chamber with a membrane with Matrigel solution (BD Biosciences, CA, USA). The same number of cells was applied to anon-coated membrane for migration assay. 750  $\mu$ l of culture medium plus 10% FBS in lower chamber was inserted into a 24-well. Following 24 h of incubation, the cells were removed from the membrane surface with cotton swabs, and the cells on the bottom surface were subjected to the fixation in 4% formaldehyde and staining with 0.5% crystal violet (Beyotime, China). The colonies from six fields per well were photographed and counted.

### In vivo experiments

Ten 6-weeks-old male BALB/c nude mice were ordered from the Shanghai Experimental Animal Center. Each of them was subcutaneously injected with  $3 \times 10^6$  Huh7 wide-type cells or PITPNA-AS1 knockdown cells. The padding was replaced every three days. To keep the

indoor air fresh, the concentration of ammonia was maintained lower than 20 ppm, and the air was changed 10~20 times per hour. The temperature was 18–22°C and the humidity was 50~60%. tumor volumes were calculated every 7 days based on the formula: Tumor volume (mm<sup>3</sup>) = (width) × (height)<sup>2</sup>/2. After 28 days, the mice were euthanized with intraperitoneal injection of 150 mg/kg sodium pentobarbital. Tumors were collected and weighed.

### Luciferase reporter assays

Cells (3 × 10<sup>4</sup>/well) transfected with wild-type (WT) or mutant (MUT) PITPNA-AS1/PDGF $\beta$  reporter were seeded in 24-well plates. Then luciferase activities of the cells were measured using a Dual-Luciferase Reporter Assay System (Promega, WI, USA).

### RNA immunoprecipitation (RIP) assay

Biotinylated PITPNA-AS1 and negative control oligo were synthesized by GenePharma Company (Shanghai, China) The RNA immunoprecipitation assay was implemented with the EZ-Magna RIP RNA-binding protein immunoprecipitation kit (Millipore, MA, USA).

### Western blot analysis

The crude proteins extracted by RIPA lysis buffer (Beyotime, China) were applied to SDS-PAGE. After electrophoresis, the separated proteins were transblotted onto a polyvinylidene difluoride membranes (Millipore, MA, USA). After blocking with 5% skim milk for 1 h, the PVDF membrane were treated with primary antibodies at 4°C overnight (E-cadherin, ab40772, dilution 1:5000; N-cadherin, ab76011, dilution 1:5000; MM9, ab76003, dilution 1:1000; MMP2, ab92536, dilution 1:1000;  $\beta$ -catenin, ab32572, dilution 1:5000; GAPDH, ab181602, dilution 1:10000). Next, the membrane was treated with respective secondary antibodies. The blot was finally developed by the Immobilon Western Chemiluminescent HRP Substrate Kit (Millipore, MA, USA). All antibodies were commercially provided by Abcam (Cambridge, UK).

### Immunohistochemistry assay (IHC)

The protocol of IHC was described previously [36]. Sections were prepared in 10  $\mu$ m. The primary antibodies against  $\beta$ -catenin (Abcam, #ab16051, 1:1000), Ki67 (Abcam, #ab245113, 1:1000), PDGF $\beta$ , E-cadherin (Abcam, #ab1416, 1:500), and N-cadherin (Abcam, #ab76057, 1:1000) were used. Following PBS washes, secondary antibodies (1:1000 was applied to sections. Lastly, the signal was developed by DAB and validated by two experienced pathologists.

### Statistical analysis

Kaplan–Meier curve and log-rank test were employed to assess the association of gene expression levels with overall survival of the patients. The significance of difference between the two groups was calculated by the student's *t*-test. The data of multi groups and time points were compared by one-way ANOVA. Statistical significance was set at *P* < 0.05. All experiment were repeated at least three times, and the data were presented as means  $\pm$  SD.

### Data availability

The data are available from the corresponding author upon reasonable request.

### AUTHOR CONTRIBUTIONS

Jianguo Yao and Xiaojian Liu conceived and supervised the project. Jianguo Yao performed the experiments. Jianguo Yao and Xiaojian Liu analyzed data and wrote the manuscript.

### CONFLICTS OF INTEREST

The authors declare no conflicts of interest related to this study.

### ETHICAL STATEMENT AND CONSENT

The present study was approved by the ethics committee of the Tongxiang First People's Hospital. Written informed consent was obtained from all patients and conducted following the Declaration of Helsinki.

### FUNDING

This work was funded by Zhejiang Medical Association Clinical Research Fund Project (2016ZYC-B13).

### REFERENCES

1. Torre LA, Bray F, Siegel RL, Ferlay J, Lortet-Tieulent J, Jemal A. Global cancer statistics, 2012. *CA Cancer J Clin.* 2015; 65:87–108. <https://doi.org/10.3322/caac.21262> PMID:[25651787](https://pubmed.ncbi.nlm.nih.gov/25651787/)
2. Siegel RL, Miller KD, Jemal A. Cancer statistics, 2019. *CA Cancer J Clin.* 2019; 69:7–34. <https://doi.org/10.3322/caac.21551> PMID:[30620402](https://pubmed.ncbi.nlm.nih.gov/30620402/)
3. Forner A, Bruix J. Biomarkers for early diagnosis of hepatocellular carcinoma. *Lancet Oncol.* 2012; 13:750–1.

[https://doi.org/10.1016/S1470-2045\(12\)70271-1](https://doi.org/10.1016/S1470-2045(12)70271-1)  
PMID:22738800

4. Aldrighetti L, Pulitanò C, Catena M, Arru M, Guzzetti E, Halliday J, Ferla G. Liver resection with portal vein thrombectomy for hepatocellular carcinoma with vascular invasion. *Ann Surg Oncol*. 2009; 16:1254.  
<https://doi.org/10.1245/s10434-009-0383-y>  
PMID:19277788
5. Yang PC, Ho CM, Hu RH, Ho MC, Wu YM, Lee PH. Prophylactic liver transplantation for high-risk recurrent hepatocellular carcinoma. *World J Hepatol*. 2016; 8:1309–17.  
<https://doi.org/10.4254/wjh.v8.i31.1309>  
PMID:27872682
6. Hombach S, Kretz M. Non-coding RNAs: Classification, Biology and Functioning. *Adv Exp Med Biol*. 2016; 937:3–17.  
[https://doi.org/10.1007/978-3-319-42059-2\\_1](https://doi.org/10.1007/978-3-319-42059-2_1)  
PMID:27573892
7. Lorenzi L, Avila Cobos F, Decock A, Everaert C, Helsemoortel H, Lefever S, Verboom K, Volders PJ, Speleman F, Vandesompele J, Mestdagh P. Long noncoding RNA expression profiling in cancer: Challenges and opportunities. *Genes Chromosomes Cancer*. 2019; 58:191–9.  
<https://doi.org/10.1002/gcc.22709>  
PMID:30461116
8. Yan G, Chang Z, Wang C, Gong Z, Xin H, Liu Z. LncRNA ILF3-AS1 promotes cell migration, invasion and EMT process in hepatocellular carcinoma via the miR-628-5p/MEIS2 axis to activate the Notch pathway. *Dig Liver Dis*. 2022; 54:125–35.  
<https://doi.org/10.1016/j.dld.2021.04.036>  
PMID:34053876
9. Liu S, Bu X, Kan A, Luo L, Xu Y, Chen H, Lin X, Lai Z, Wen D, Huang L, Shi M. SP1-induced lncRNA DUBR promotes stemness and oxaliplatin resistance of hepatocellular carcinoma via E2F1-CIP2A feedback. *Cancer Lett*. 2022; 528:16–30.  
<https://doi.org/10.1016/j.canlet.2021.12.026>  
PMID:34958891
10. Zhong F, Liu S, Hu D, Chen L. LncRNA AC099850.3 promotes hepatocellular carcinoma proliferation and invasion through PRR11/PI3K/AKT axis and is associated with patients prognosis. *J Cancer*. 2022; 13:1048–60.  
<https://doi.org/10.7150/jca.66092>  
PMID:35154469
11. Wang F, Zhu L, Xue Q, Tang C, Tang W, Zhang N, Dai C, Chen Z. Novel lncRNA AL033381.2 Promotes Hepatocellular Carcinoma Progression by Upregulating PRKRA Expression. *Oxid Med Cell Longev*. 2022; 2022:1125932.  
<https://doi.org/10.1155/2022/1125932>  
PMID:35035655
12. Haemmerle M, Gutschner T. Long non-coding RNAs in cancer and development: where do we go from here? *Int J Mol Sci*. 2015; 16:1395–405.  
<https://doi.org/10.3390/ijms16011395>  
PMID:25580533
13. Derrien T, Johnson R, Bussotti G, Tanzer A, Djebali S, Tilgner H, Guernec G, Martin D, Merkel A, Knowles DG, Lagarde J, Veeravalli L, Ruan X, et al. The GENCODE v7 catalog of human long noncoding RNAs: analysis of their gene structure, evolution, and expression. *Genome Res*. 2012; 22:1775–89.  
<https://doi.org/10.1101/gr.132159.111>  
PMID:22955988
14. Geisler S, Collier J. RNA in unexpected places: long non-coding RNA functions in diverse cellular contexts. *Nat Rev Mol Cell Biol*. 2013; 14:699–712.  
<https://doi.org/10.1038/nrm3679>  
PMID:24105322
15. Hansen TB, Jensen TI, Clausen BH, Bramsen JB, Finsen B, Damgaard CK, Kjems J. Natural RNA circles function as efficient microRNA sponges. *Nature*. 2013; 495:384–8.  
<https://doi.org/10.1038/nature11993>  
PMID:23446346
16. Liu Y, Geng X. Long non-coding RNA (lncRNA) CYTOR promotes hepatocellular carcinoma proliferation by targeting the microRNA-125a-5p/LASP1 axis. *Bioengineered*. 2022; 13:3666–79.  
<https://doi.org/10.1080/21655979.2021.2024328>  
PMID:35081873
17. Sun J, Zhang Y, Li B, Dong Y, Sun C, Zhang F, Jin L, Chen D, Wang W. PIPNA-AS1 abrogates the inhibition of miR-876-5p on WNT5A to facilitate hepatocellular carcinoma progression. *Cell Death Dis*. 2019; 10:844.  
<https://doi.org/10.1038/s41419-019-2067-2>  
PMID:31700026
18. Guo Q, Li L, Bo Q, Chen L, Sun L, Shi H. Long noncoding RNA PIPNA-AS1 promotes cervical cancer progression through regulating the cell cycle and apoptosis by targeting the miR-876-5p/c-MET axis. *Biomed Pharmacother*. 2020; 128:110072.  
<https://doi.org/10.1016/j.biopha.2020.110072>  
PMID:32460193
19. Wang QF, Wang QL, Cao MB. LncRNA PIPNA-AS1 as a Potential Diagnostic Marker and Therapeutic Target Promotes Hepatocellular Carcinoma Progression via Modulating miR-448/ROCK1 Axis. *Front Med (Lausanne)*. 2021; 8:668787.  
<https://doi.org/10.3389/fmed.2021.668787>  
PMID:34055841

20. Dong ZB, Wu HM, He YC, Huang ZT, Weng YH, Li H, Liang C, Yu WM, Chen W. MiRNA-124-3p.1 sensitizes hepatocellular carcinoma cells to sorafenib by regulating FOXO3a by targeting AKT2 and SIRT1. *Cell Death Dis.* 2022; 13:35. <https://doi.org/10.1038/s41419-021-04491-0> PMID:35013144
21. Tan W, Li Z, Xia W, Zhu J, Fan R. miR-221-3p regulates hepatocellular carcinoma cell proliferation, migration and invasion via targeting LIFR. *Ann Hepatol.* 2022 (Suppl 1); 27:100567. <https://doi.org/10.1016/j.aohep.2021.100567> PMID:34699986
22. Nakano K, Miki Y, Hata S, Ebata A, Takagi K, McNamara KM, Sakurai M, Masuda M, Hirakawa H, Ishida T, Suzuki T, Ohuchi N, Sasano H. Identification of androgen-responsive microRNAs and androgen-related genes in breast cancer. *Anticancer Res.* 2013; 33:4811–9. PMID:24222117
23. Zhang J, Fan J, Zhou C, Qi Y. miR-363-5p as potential prognostic marker for hepatocellular carcinoma indicated by weighted co-expression network analysis of miRNAs and mRNA. *BMC Gastroenterol.* 2017; 17:81. <https://doi.org/10.1186/s12876-017-0637-2> PMID:28637446
24. Wang X, Qian T, Bao S, Zhao H, Chen H, Xing Z, Li Y, Zhang M, Meng X, Wang C, Wang J, Gao H, Liu J, et al. Circulating exosomal miR-363-5p inhibits lymph node metastasis by downregulating PDGFB and serves as a potential noninvasive biomarker for breast cancer. *Mol Oncol.* 2021; 15:2466–79. <https://doi.org/10.1002/1878-0261.13029> PMID:34058065
25. Chen G, Sun W, Hua X, Zeng W, Yang L. Long non-coding RNA FOXD2-AS1 aggravates nasopharyngeal carcinoma carcinogenesis by modulating miR-363-5p/S100A1 pathway. *Gene.* 2018; 645:76–84. <https://doi.org/10.1016/j.gene.2017.12.026> PMID:29248577
26. Wang KC, Chang HY. Molecular mechanisms of long noncoding RNAs. *Mol Cell.* 2011; 43:904–14. <https://doi.org/10.1016/j.molcel.2011.08.018> PMID:21925379
27. Sun W, Yang Y, Xu C, Guo J. Regulatory mechanisms of long noncoding RNAs on gene expression in cancers. *Cancer Genet.* 2017; 216-217:105–10. <https://doi.org/10.1016/j.cancergen.2017.06.003> PMID:29025584
28. Adams BD, Kasinski AL, Slack FJ. Aberrant regulation and function of microRNAs in cancer. *Curr Biol.* 2014; 24:R762–76. <https://doi.org/10.1016/j.cub.2014.06.043> PMID:25137592
29. Hou C, Wang X, Du B. lncRNA MCM3AP-AS1 promotes the development of oral squamous cell carcinoma by inhibiting miR-363-5p. *Exp Ther Med.* 2020; 20:978–84. <https://doi.org/10.3892/etm.2020.8738> PMID:32742341
30. Ying J, Yu X, Ma C, Zhang Y, Dong J. MicroRNA-363-3p is downregulated in hepatocellular carcinoma and inhibits tumorigenesis by directly targeting specificity protein 1. *Mol Med Rep.* 2017; 16:1603–11. <https://doi.org/10.3892/mmr.2017.6759> PMID:28627662
31. Wu Q, Wang R, Yang Q, Hou X, Chen S, Hou Y, Chen C, Yang Y, Miele L, Sarkar FH, Chen Y, Wang Z. Chemoresistance to gemcitabine in hepatoma cells induces epithelial-mesenchymal transition and involves activation of PDGF-D pathway. *Oncotarget.* 2013; 4:1999–2009. <https://doi.org/10.18632/oncotarget.1471> PMID:24158561
32. Kong D, Li Y, Wang Z, Banerjee S, Ahmad A, Kim HR, Sarkar FH. miR-200 regulates PDGF-D-mediated epithelial-mesenchymal transition, adhesion, and invasion of prostate cancer cells. *Stem Cells.* 2009; 27:1712–21. <https://doi.org/10.1002/stem.101> PMID:19544444
33. Wang Z, Ahmad A, Li Y, Kong D, Azmi AS, Banerjee S, Sarkar FH. Emerging roles of PDGF-D signaling pathway in tumor development and progression. *Biochim Biophys Acta.* 2010; 1806:122–30. <https://doi.org/10.1016/j.bbcan.2010.04.003> PMID:20434526
34. Wu Q, Hou X, Xia J, Qian X, Miele L, Sarkar FH, Wang Z. Emerging roles of PDGF-D in EMT progression during tumorigenesis. *Cancer Treat Rev.* 2013; 39:640–6. <https://doi.org/10.1016/j.ctrv.2012.11.006> PMID:23261166
35. Wu Z, Huang W, Wang X, Wang T, Chen Y, Chen B, Liu R, Bai P, Xing J. Circular RNA CEP128 acts as a sponge of miR-145-5p in promoting the bladder cancer progression via regulating SOX11. *Mol Med.* 2018; 24:40. <https://doi.org/10.1186/s10020-018-0039-0> PMID:30134837
36. Zeng K, Chen X, Xu M, Liu X, Hu X, Xu T, Sun H, Pan Y, He B, Wang S. CircHIPK3 promotes colorectal cancer growth and metastasis by sponging miR-7. *Cell Death Dis.* 2018; 9:417. <https://doi.org/10.1038/s41419-018-0454-8> PMID:29549306